



# Supersalts $\text{Na}_2\text{MgX}_4$ ( $X = \text{F}, \text{Cl}$ ): Quantum Chemical Study of the Structure, Vibration Spectra and Thermodynamic Properties

Evance A. Ulime<sup>1\*</sup>, Alexander M. Pogrebnoi<sup>1</sup> and Tatiana P. Pogrebnaya<sup>1</sup>

<sup>1</sup>Department of Materials, Energy Science and Engineering, The Nelson Mandela African Institution of Science and Technology (NM-AIST), Arusha, Tanzania.

## Authors' contributions

This work was carried out in collaboration between all authors. Author EAU performed computations, wrote the first draft of the manuscript and managed literature searches. Author AMP performed some selected computations of thermodynamic properties. Author TPP performed corrections and some selected computations regarding the structure and vibrational spectra. All authors analyzed and discussed the results and approved the final manuscript.

## Article Information

DOI: 10.9734/BJAST/2016/21677

### Editor(s):

(1) Jon S. Gold, Dept. of Chemistry, East Stroudsburg University, East Stroudsburg, PA, USA.

### Reviewers:

(1) Anonymous, University of Missouri-St. Louis, USA.

(2) Alexandre Gonçalves Pinheiro, Universidade Estadual do Ceará, Quixadá, Brazil.

Complete Peer review History: <http://sciencedomain.org/review-history/11672>

Original Research Article

Received 28<sup>th</sup> August 2015  
Accepted 19<sup>th</sup> September 2015  
Published 5<sup>th</sup> October 2015

## ABSTRACT

The theoretical study of supersalts  $\text{Na}_2\text{MgX}_4$  ( $X = \text{F}, \text{Cl}$ ) has been performed. The formation of the supersalts was considered through association reactions between different building blocks: superalkalies and superhalogens, ionic ( $\text{Na}_2\text{X}^+$  and  $\text{MgX}_3^-$ ) and neutral ( $\text{Na}_2\text{X}$  and  $\text{MgX}_3$ ), as well as dimers  $\text{Na}_2\text{X}_2$  and traditional salts  $\text{MgX}_2$ . The optimization of geometrical structures, and determination of vibrational spectra of supersalts and their respective building blocks was carried out by the DFT/B3P86 and MP2 methods; the McLean–Chandler basis set and the extended basis set (cc-pVTZ for Na, Mg; aug-cc-pVTZ for F, Cl) were used. Different possible geometrical configurations for  $\text{Na}_2\text{MgX}_4$  were considered, among which two structures: two-cycled structure of  $D_{2d}$  symmetry and polyhedral,  $C_{2v}$ , were proved to be isomers; their relative concentrations in equilibrium vapour were evaluated. The energies and enthalpies of the association reactions were determined. The enthalpies of formation  $\Delta_f H^\circ(0)$  of gas-phase supersalts found as follows:  $-1850 \pm 30 \text{ kJ}\cdot\text{mol}^{-1}$  ( $\text{Na}_2\text{MgF}_4$ ) and  $-1170 \pm 40 \text{ kJ}\cdot\text{mol}^{-1}$  ( $\text{Na}_2\text{MgCl}_4$ ).

\*Corresponding author: E-mail: [ulimee@nm-aist.ac.tz](mailto:ulimee@nm-aist.ac.tz)

**Keywords:** Supersalt; superatom; superhalogen; superalkali; geometrical structure; vibrational spectrum; enthalpy of formation.

## 1. INTRODUCTION

The critical investigation, prediction and understanding of the structure and a wide range of the properties of individual components of a given substance not only are a crucial and continuous, but also a very important aspect towards designing and development of chemical species with outstanding properties. Khanna and Jena [1,2] proposed and pioneered on the existence of superatoms which are defined as clusters of atoms with suitable size and composition that can mimic the chemistry of atoms in the periodic table. Being experienced players in the field of computational chemistry, Gutsev and Bodyrev [3] classified superatoms as ‘Superhalogens’, chemical species with higher electron affinity (*EA*) than that of chlorine (3.6 eV), and ‘Superalkali’, chemical species with lower ionization potentials than normal alkali metals. Simple examples of superalkali and superhalogen are  $M_2X$  and  $MX_2$  respectively where *M* is the alkali metal and *X* is halogen. The technique used in designing superatoms is by combining the most electronegative group VII elements with the most electropositive group I elements in the right and reasonable proportions. And according to Tian [4], the superatoms are very important as they provide compounds with novel structures, novel properties and special binding nature which all together contribute to, and promote the development of chemistry.

A little progress has already been made in the research of supersalts, and the recent studies include the novel  $Li_3X_3$  supersalt by Srivastava and Misra[5], and different supersalts by Giri [6]. But both have described only the electron affinity, ionization potential, and binding energies of the supersalts.

This theoretical study intends to design and optimize the geometrical structure of  $Na_2MgX_4$  (*X* = F, Cl) supersalts. A design of these species is considered through interaction of different building blocks: superalkalies and superhalogens, ionic ( $Na_2X^+$  and  $MgX_3^-$ ) and neutral ( $Na_2X$  and  $MgX_3$ ), as well as dimers  $Na_2X_2$  and traditional salts  $MgX_2$ . The work also is aimed to examine critically the vibrational spectra and thermodynamic properties of supersalts, superatoms and traditional salts.

## 2. COMPUTATIONAL DETAILS

All calculations have been carried out by using the PC GAMESS program (Firefly 8.1.0 version) [7,8]. The methods used were the density functional theory (DFT/B3P86) and the Møller–Plesset perturbation theory of second order (MP2). Two basis sets have been employed: the first one was McLean–Chandler basis set (MC) with *d*-functions added for all atoms [9,10], and second (called hereafter the “extended” and denoted as Ext): cc-pVTZ for metals and aug-cc-pVTZ for halogens [11]. For MP2 method, no frozen AO (NCORE=0) were considered for fluorides and 1s AO of Cl atom were frozen for chlorine containing species.

The geometry of the species was optimized using B3P86 and MP2 methods with both basis sets. The vibrational analysis was performed at the same level to verify that all obtained structures correspond to a real minimum energy by the absence of imaginary frequencies. Geometrical structures were analyzed and examined by using the Chemcraft software [12] as a visualization tool.

The thermodynamic functions were determined in the rigid rotator-harmonic oscillator approximation using the Openthermo software [13]. The required reference data for the thermodynamic calculations were taken from [14]. The values of enthalpies of reactions  $\Delta_r H^\circ(0)$  were computed theoretically using the formulae:

$$\Delta_r H^\circ(0) = \Delta_r E + \Delta_r \epsilon \quad (1)$$

$$\Delta_r \epsilon = 1/2hc (\sum \omega_{i, \text{product}} - \sum \omega_{i, \text{reactant}}) \quad (2)$$

Where  $\Delta_r E$  is the energy of the reaction calculated through the total energies *E* of the species,  $\Delta_r \epsilon$  is the zero point vibration energy correction,  $\sum \omega_{i, \text{prod}}$  and  $\sum \omega_{i, \text{reactant}}$  are the sums of the vibration frequencies of the products and reactants respectively.

## 3. RESULTS AND DISCUSSION

### 3.1 Analysis of the Computational Approaches

To analyze the accuracy of the calculated properties for the supersalts, the related species

NaX, MgX<sub>2</sub>, and dimers Na<sub>2</sub>X<sub>2</sub> (X = F, Cl) were considered and their properties were computed and compared with experimental data. The four theoretical approaches B3P86 MC, MP2 MC, B3P86 Ext, MP2 Ext were applied. The ionization energies and electron affinities were calculated as the energy difference  $\Delta E$  between the ionic and neutral states. For the adiabatic values, the optimized coordinates were used for both states. For vertical magnitudes the parameters were optimized for the singlet-state species only, while for doublet-states the same parameters were accepted. The adiabatic values were computed by DFT method only as MP2 suffers from the spin contamination [15,16] and the optimization procedure for molecules with multiplicity more than one was not incorporated in the software used.

The results for NaX molecules are given in Table 1. It is seen that for both molecules NaF and NaCl the internuclear distances,  $R_e$ , found theoretically by four methods do not contradict the literature data, the difference does not exceed 0.02 Å. For both NaX molecules, the B3P86 Ext and MP2 Ext methods gave better vibrational frequencies in accordance with the reference values. Regarding the dipole moment, the results by the B3P86 Ext level are in the best agreement with the reference data [17]. For the ionization energies, MP2 Ext produces the values which are most close to the literature

data. The calculated electron affinities are in accordance with the reference EAs.

The results for the MgX<sub>2</sub> molecules are presented in Table 2. There is no clear-cut preference in theoretical values of inter nuclear separations, vibrational frequencies and ionization energies found by DFT and MP2 methods, although the results by B3P86 are in better agreement with experimental data.

For the dimer molecules Na<sub>2</sub>F<sub>2</sub> and Na<sub>2</sub>Cl<sub>2</sub> the equilibrium geometry ( $D_{2h}$  symmetry) is presented in Fig. 1(a) and the calculated parameters are given in Table 3. The experimental data on the geometrical parameters of these molecules are not available and the fundamental frequencies are scarce. The parameters calculated by different methods agree well with each other, the difference does not exceed 0.02–0.03 Å for  $R_e$  (Na-X), 2° for valence angle  $\alpha_e$ (Na-X-Na), and ~10% for vibrational frequencies. As compared to the experimental frequencies, the B3P86 Ext approach looks preferable.

The energies of the dimerization reactions  $2\text{NaX} = \text{Na}_2\text{X}_2$  were determined through the total energies of the species. The enthalpies of the reactions presented in Table 3 were calculated using Eqs. (1) and (2). Fig. 2 presents the enthalpies of reactions together with the reference values.

**Table 1. Comparison of the calculated properties of NaX (X = F, Cl) with the reference data**

Property	B3P86 MC	MP2 MC	B3P86 Ext	MP2 Ext	Expt [17]
<b>NaF</b>					
$R_e$	1.918	1.929	1.941	1.937	1.926
$-E$	262.13604	261.72199	262.16684	261.71972	
$\mu_e$	9.51	7.73	8.17	11.09	8.16
$IE_{\text{vert}}$	10.10	9.65	10.33	10.40	10.88
$IE_{\text{ad}}$	9.66		9.96		10.88
$EA_{\text{ad}}$	0.56		0.65		0.52
$\omega_e$	564	562	520	525	535.7
<b>NaCl</b>					
$R_e$	2.381	2.373	2.379	2.374	2.361
$-E$	622.53227	621.74517	622.55180	621.74107	
$\mu_e$	9.53	9.13	8.99	9.18	9.00
$IE_{\text{vert}}$	9.38	8.77	9.36	9.21	9.20
$IE_{\text{ad}}$	9.15		9.13		9.20
$EA_{\text{ad}}$	0.86		0.87		0.73
$\omega_e$	355	374	352	358	364

Notes: Here and hereafter in Tables 2–7,  $R_e$  is the internuclear distance in Å;  $E$  is the total energy in au,  $\mu_e$  is the dipole moment in D;  $IE_{\text{vert}}$ ,  $IE_{\text{ad}}$ , and  $EA_{\text{ad}}$  are the ionization energies, vertical and adiabatic, and electron affinity in eV,  $\omega_e$  is the fundamental frequency in  $\text{cm}^{-1}$

**Table 2. Comparison of the calculated properties of MgX<sub>2</sub> (X = F, Cl) with the reference data**

Property	B3P86 MC	MP2 MC	B3P86 Ext	MP2 Ext	Expt
<b>MgF<sub>2</sub>(D<sub>∞h</sub>)</b>					
R <sub>e</sub>	1.759	1.764	1.751	1.735	1.77[18]
-E	399.86786	399.29947	399.90604	399.38344	
IE <sub>vert</sub>	13.31	14.30	13.35	14.83	13.60 [19]
IE <sub>ad</sub>	13.22		13.35		13.60[19]
EA <sub>ad</sub>	0.27		0.53		
ω <sub>1</sub> (Σ <sub>g</sub> <sup>+</sup> )	567	567	560	548	540 [18]
ω <sub>2</sub> (Σ <sub>u</sub> <sup>+</sup> )	905	908	882	863	825 [18]
ω <sub>3</sub> (Π <sub>u</sub> )	141	130	166	155	165 [18]
<b>MgCl<sub>2</sub>(D<sub>∞h</sub>)</b>					
R <sub>e</sub>	2.188	2.180	2.177	2.173	2.18[20]
-E	1120.60967	1119.29589	1120.63482	1119.37735	
IE <sub>vert</sub>	12.12	12.36	12.02	12.66	11.58[20]
IE <sub>ad</sub>	12.08		11.99		11.58[20]
EA <sub>ad</sub>	0.78		0.81		
ω <sub>1</sub> (Σ <sub>g</sub> <sup>+</sup> )	317	329	314	315	320 [20]
ω <sub>2</sub> (Σ <sub>u</sub> <sup>+</sup> )	612	635	613	619	596 [20]
ω <sub>3</sub> (Π <sub>u</sub> )	111	109	111	111	110 [20]

**Table 3. Calculated properties of the dimers Na<sub>2</sub>X<sub>2</sub>**

Property	B3P86 MC	MP2 MC	B3P86 Ext	MP2 Ext	Reference
<b>Na<sub>2</sub>F<sub>2</sub> (D<sub>2h</sub>)</b>					
R <sub>e</sub> (Na-F)	2.063	2.077	2.081	2.068	2.094 [21]
α <sub>e</sub> (Na-F-Na)	85.7	85.8	85.0	83.3	87.1[21]
-E	524.376970	523.55503	524.424173	523.53812	
ω <sub>1</sub> (A <sub>g</sub> )	416	414	387	370	
ω <sub>2</sub> (A <sub>g</sub> )	213	214	204	186	
ω <sub>3</sub> (B <sub>1g</sub> )	367	365	338	329	
ω <sub>4</sub> (B <sub>1u</sub> )	158	157	153	152	
ω <sub>5</sub> (B <sub>2u</sub> )	390	386	361	350	363 [22]
ω <sub>6</sub> (B <sub>3u</sub> )	413	412	385	368	380 [22]
-Δ <sub>r</sub> E	275.4	291.6	237.6	259.1	
-Δ <sub>r</sub> H <sup>o</sup> (0)	268.1	286.8	232.9	254.9	242.0 [14]
<b>Na<sub>2</sub>Cl<sub>2</sub> (D<sub>2h</sub>)</b>					
R <sub>e</sub> (Na-Cl)	2.552	2.531	2.548	2.516	2.538 [21]
α <sub>e</sub> (Na-Cl-Na)	78.3	78.8	77.2	76.8	79.8 [21]
-E	1245.13954	1243.57286	1245.176890	1243.56387	
ω <sub>1</sub> (A <sub>g</sub> )	258	281	266	270	
ω <sub>2</sub> (A <sub>g</sub> )	132	133	133	122	
ω <sub>3</sub> (B <sub>1g</sub> )	233	255	232	247	
ω <sub>4</sub> (B <sub>1u</sub> )	92	95	92	90	116 [23]
ω <sub>5</sub> (B <sub>2u</sub> )	227	245	223	231	228 [23]
ω <sub>6</sub> (B <sub>3u</sub> )	278	300	278	288	274 [23]
-Δ <sub>r</sub> E	196.9	216.7	192.4	214.6	
-Δ <sub>r</sub> H <sup>o</sup> (0)	193.9	213.6	189.3	211.5	200.8 [14]

Note: Δ<sub>r</sub>E and Δ<sub>r</sub>H<sup>o</sup>(0) are the energy and enthalpy of the dimerization reactions 2NaX = Na<sub>2</sub>X<sub>2</sub>, in kJ.mol<sup>-1</sup>; α<sub>e</sub> is the bond angle in degrees

The results obtained with the extended basis sets show good accordance with reference values [14]. The calculated average values between B3P86 Ext and MP2 Ext are equal to -244±11 kJ.mol<sup>-1</sup> for Na<sub>2</sub>F<sub>2</sub> and -200±11kJ.mol<sup>-1</sup> for Na<sub>2</sub>Cl<sub>2</sub>.Uncertainties were

estimated as a half-difference between B3P86 Ext and MP2 Ext results. Both averaged values are very close to the reference data,  $-242$  and  $-200.8 \text{ kJ}\cdot\text{mol}^{-1}$  from [14], respectively.

Concluding this section, we can state that all four methods (B3P86 MC, MP2 MC, B3P86 Ext, and MP2 Ext) are suitable for the geometrical parameters and vibrational spectra

determination, while the approaches with extended basis sets, B3P86 Ext and MP2 Ext, are preferable for the calculation of enthalpies of the reactions. In order to obtain the total array of the parameters of acceptable accuracy, we assume the methods B3P86 Ext and MP2 Ext are appropriate and reliable and therefore they have been applied in computations of properties of the superatoms and supersalts.

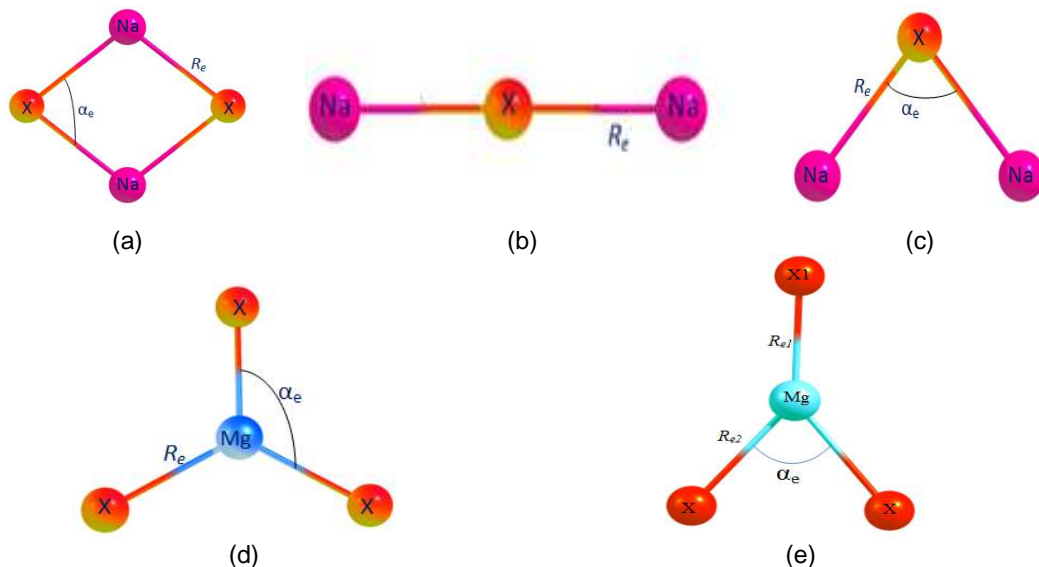


**Fig. 1. Equilibrium geometrical structures of the species: (a) dimers  $\text{Na}_2\text{X}_2$ ,  $D_{2h}$ ; (b) ionic superalkali  $\text{Na}_2\text{X}^+$ ,  $D_{\infty h}$ ; (c) neutral superalkali  $\text{Na}_2\text{X}$ ,  $C_{2v}$ ; (d) ionic superhalogens  $\text{MgX}_3^-$ ,  $D_{3h}$ ; and (e) neutral  $\text{MgX}_3$ ,  $C_{2v}$ , ( $X = \text{F}, \text{Cl}$ )**

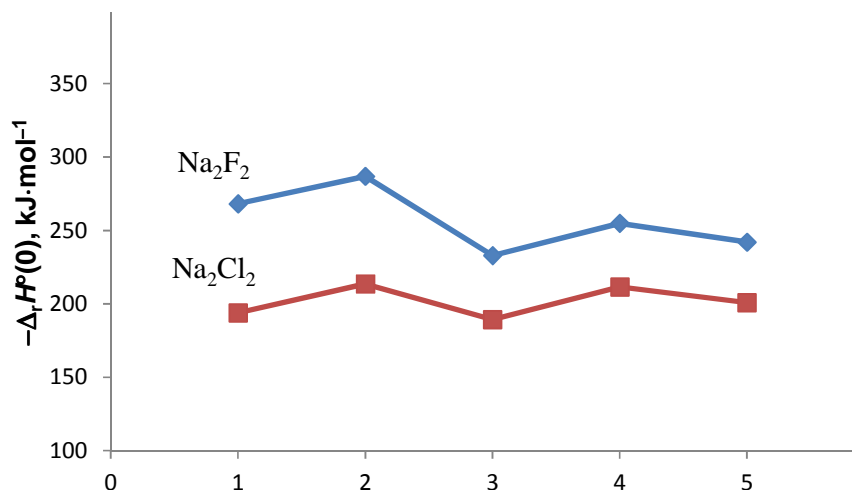


**Fig. 2. Enthalpies of dimerization reactions  $2\text{NaX} = \text{Na}_2\text{X}_2$ ,  $\Delta_r H^0(0)$  versus the level of calculations: 1 – B3P86 MC, 2 – MP2 MC, 3 – B3P86 Ext, 4 – MP2 Ext, 5 – the reference from IVTANTHERMO Database [14]**

### 3.2 Geometrical Structure and Vibration Spectra of Superalkalies and Superhalogens

#### 3.2.1 Superalkalies

The neutral and ionic superalkalies involved in this study are  $\text{Na}_2\text{F}$  and  $\text{Na}_2\text{Cl}$ , and  $\text{Na}_2\text{F}^+$  and  $\text{Na}_2\text{Cl}^+$ . Electronic state of the neutral superalkalies  $\text{Na}_2\text{X}$  is  $^2\text{A}_1$  and  $^1\text{A}_1$  for ionic  $\text{Na}_2\text{X}^+$  (B3P86 Ext). Their equilibrium geometrical structures are shown in Figs. 1 (b) and (c). The neutral superalkalies assume a bent structure while ionic,  $\text{Na}_2\text{F}^+$  and  $\text{Na}_2\text{Cl}^+$ , linear shape. Calculated geometrical parameters and vibrational frequencies of superalkalies are presented in Table 4. It is seen that for the ionic species MP2 gives the shorter values of internuclear distances, by 0.03–0.04 Å, than DFT, while the DFT results are very close to the data obtained earlier using CISD+Q method [24, 25]. At the same time the values of vibrational frequencies by both methods do not contradict the results obtained previously [23,24], a controversial result for the deformational frequency in  $\text{Na}_2\text{F}^+$  (157  $\text{cm}^{-1}$ ) found by MP2 Ext.

The bent structure of neutral superalkalies has the valence angles  $104^\circ$  and  $80^\circ$  in  $\text{Na}_2\text{F}$  and  $\text{Na}_2\text{Cl}$ , respectively. The linear structure of the neutral species  $\text{Na}_2\text{X}$  has also been taken into consideration and this structure had a higher energy by 7  $\text{kJ}\cdot\text{mol}^{-1}$  for  $\text{Na}_2\text{F}$  and 19  $\text{kJ}\cdot\text{mol}^{-1}$  for  $\text{Na}_2\text{Cl}$ , moreover the imaginary frequencies were

found for the linear structure that indicates non equilibrium state. A significant difference in vibrational frequencies is noted between ionic and neutral clusters especially for the  $\text{Na}_2\text{Cl}^+$  and  $\text{Na}_2\text{Cl}$  species. This might be accounted by the influence of the one extra electron in ionic clusters as compared to their respective neutral species and change in geometrical structure from linear for ions to bent for neutrals.

Adiabatic ionization energies ( $IE_{ad}$ ) of neutral clusters were obtained by B3P86 Ext as the energy difference  $\Delta E$  between their neutral and ionic states with optimized structures. For the MP2 method, there was no optimization of the neutral  $\text{Na}_2\text{X}$ , consequently only estimation of the  $IP_{vert}$  values was done. The ionization energies of the  $\text{Na}_2\text{X}$  species was found to be lower than that of Na (5.14 eV) hence they proved to be typical superalkalies and suitable reducing agents.

#### 3.2.2 Superhalogens

The equilibrium geometrical structures of the ionic and neutral superhalogens;  $\text{MgX}_3^-$  and  $\text{MgX}_3$  are presented by Fig. 1d, e. The structure of the ionic species is of  $D_{3h}$  symmetry, while that of neutral is of  $C_{2v}$  symmetry. The parameters are shown in Table 5. From the ionic state to neutral, the symmetry is lowered, the geometrical parameters: bond lengths and valence angles becomes non-equivalent (Fig. 1 e). For  $\text{MgCl}_3^-$  the internuclear distance and vibrational frequencies are in agreement with the values obtained by CCSD(T)/6-311+G\* [26].

Table 4. Calculated properties of superalkalies  $\text{Na}_2\text{X}$  (X=F, Cl)

Property	B3P86 Ext	MP2 Ext	[24]	B3P86 Ext	MP2 Ext	[25]
	$\text{Na}_2\text{F}^+(D_{\infty h}, ^1A_1)$			$\text{Na}_2\text{Cl}^+(D_{\infty h}, ^1A_1)$		
$R_e(\text{Na-X})$	2.024	1.985	2.033	2.480	2.450	2.483
$-E$	424.32459	423.53076	423.57148	784.68892	783.52799	783.56586
$\omega_1(\Sigma_g^+)$	290	290	290	219	227	230
$\omega_2(\Sigma_u^+)$	512	534	518	324	339	334
$\omega_3(\Pi_u)$	106	157	118	43	54	51(2)
$\text{Na}_2\text{F}(C_{2v}, ^2A_1)$				$\text{Na}_2\text{Cl}(C_{2v}, ^2A_1)$		
$R_e(\text{Na-X})$	2.047	(2.047)		2.543	(2.543)	
$\alpha_e(\text{Na-X-Na})$	104.3	(104.3)		79.5	(79.5)	
$-E$	424.46869	423.65677		784.84058	783.66550	
$IE_{ad}$	3.92			4.13		
$IE_{vert}$		3.43			3.74	
$\omega_1(A_1)$	374			266		
$\omega_3(A_1)$	96			106		
$\omega_2(B_1)$	396			214		

Electronic state of the ionic superhalides is  $^1A_1$  for both  $MgX_3^-$  and  $^2B_2$  and  $^2A_1$  for neutral  $MgF_3$  and  $MgCl_3$ , respectively (B3P86 Ext). The values of vertical energy detachment (VED) of electron from anion  $MgX_3^-$  were found using the MP2 Ext level, the geometrical parameters for the neutral  $MgX_3$  were accepted the same as those optimized for the ionic  $MgX_3^-$  species (both neutral and anionic are of  $D_{3h}$ ). The value 6.64 eV for the  $MgCl_3^-$  agrees well with the experimental result  $6.60 \pm 0.04$  eV [26]. The theoretical result 6.50 eV [26] corresponds to the state  $^2B_2$  of  $MgCl_3$  determined which is different from ours,  $^2A_1$ .

Adiabatic electron affinities of neutral  $MgX_3$  were also calculated by B3P86 method. For  $MgF_3$  EA is noticeably higher than for  $MgCl_3$ , 6.93 and 6.21 eV, respectively. These results prove that these molecules release much energy when they accept electrons *i.e.* have high EA as compared to normal halogens, 3.4 eV (F) and 3.6 eV (Cl).

### 3.3 Geometrical Structure and Vibration Spectra of Supersalts $Na_2MgX_4$

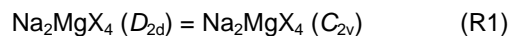
Different geometrical shapes of the  $Na_2MgX_4$  molecules have been considered: a structure with two cycles in perpendicular planes of  $D_{2d}$  symmetry, polyhedral compact structure,  $C_{2v}$ , and bipyramidal one with a tail,  $C_{3v}$ . Among these configurations, the first two were proved to correspond to the minima at the potential energy surface. The optimized equilibrium geometrical structures of supersalts  $Na_2MgX_4$  are shown and specified in Fig. 3.

The geometrical parameters and fundamental frequencies for isomers  $D_{2d}$  and  $C_{2v}$  computed by B3P86 and MP2 method with the extended basis set are gathered in Tables 6 and 7 respectively. The corresponding geometrical parameters obtained by the two methods agree in general between each other; for instance the DFT  $R_e$  values are longer than MP2 values by 0.01–0.03 Å.

The IR spectra (MP2 Ext) are presented in Fig. 4. The similarity of the vibrational bands is observed for  $Na_2MgF_4$  and  $Na_2MgCl_4$  for isomers of the same configurations. For example, in the spectra of the  $D_{2d}$  isomers, the most intensive bands correspond to the Mg-X asymmetrical stretching vibrations at  $521\text{ cm}^{-1}$  ( $Na_2MgF_4$ ) and  $360\text{ cm}^{-1}$  ( $Na_2MgCl_4$ ). The high intensities of bands assigned to Mg-X modes are caused by

the bigger number of Mg-X bonds compared to Na-X; in both isomers Mg atom links with four X atoms while Na atom, being the terminal, forms two bonds in  $D_{2d}$  and three in  $C_{2v}$ . The valence vibrations of Mg-X bonds are of higher frequency than those of Na-X; e.g. in the spectrum of  $Na_2MgF_4$  ( $D_{2d}$ ), the bands at 619 and  $521\text{ cm}^{-1}$  are assigned to Mg-F stretching modes whereas 376 and 330 correspond to Na-F stretching vibrations (Fig. 4a). The similar relationship is observed in spectrum of  $Na_2MgCl_4$  ( $D_{2d}$ ), Fig. 4b, as well in spectra of both  $C_{2v}$   $Na_2MgF_4$  and  $Na_2MgCl_4$  isomers (Figs. 4 c, d). This relationship connects to the internuclear separations between metal and halide, shorter the distance higher is the frequency.

To evaluate the concentration of two isomers in the equilibrium vapour, the isomerization reactions



were considered. The isomerization energies  $\Delta_r E_{iso}$  were calculated by equation

$$\Delta_r E_{iso} = E(C_{2v}) - E(D_{2d}) \quad (3)$$

and given in Table 7. The values of  $\Delta_r E_{iso}$  are negative:  $-13\text{ kJ mol}^{-1}$  ( $Na_2MgF_4$ ) and  $-23\text{ kJ mol}^{-1}$  ( $Na_2MgCl_4$ ), according to MP2 Ext calculations; therefore the  $C_{2v}$  isomer is more stable energetically as compared to  $D_{2d}$  isomer for both species. Their relative abundance in saturated vapour was estimated using the following equation:

$$\Delta_r H^\circ(0) = T\Delta_r \Phi^\circ(T) - RT \ln \left( \frac{p_{II}}{p_I} \right), \quad (4)$$

where  $\Delta_r H^\circ(0)$  is the enthalpy of the reaction;  $T$  is absolute temperature;  $\Delta_r \Phi^\circ(T)$  is the change in the reduced Gibbs energy of the reaction,  $\Phi^\circ(T) = -[H^\circ(T) - H^\circ(0) - TS^\circ(T)]/T$ ;  $p_{II}/p_I$  is the pressure ratio between two isomers, isomer I corresponds to  $D_{2d}$ , and II corresponds to  $C_{2v}$ . Thermodynamic functions of the isomers are given in Appendix. The enthalpies of the isomerization reactions  $\Delta_r H^\circ(0)$  were calculated using isomerization energies  $\Delta_r E$  and the ZPVE corrections  $\Delta_r \epsilon$  as given in Eqs. (1) and (2). The values of  $\Phi^\circ(T)$  were calculated using the optimized coordinates and vibrational frequencies obtained by MP2 method with extended basis set. The relative concentrations have been calculated for the temperature range 700 – 1600 K and the plots are displayed in Fig. 5.

The results show that the two isomers  $C_{2v}$  and  $D_{2d}$  are of comparable amount in a broad temperature range. For example, at 1000 K the value of  $\rho_{II}/\rho_I$  equals to  $\sim 1.2$  and  $\sim 0.5$  for  $Na_2MgF_4$  and  $Na_2MgCl_4$ , respectively. The isomer of the compact structure ( $C_{2v}$ ) prevails at temperature below  $\sim 1100$  K for  $Na_2MgF_4$  and at  $T < 800$  K for  $Na_2MgCl_4$ . With temperature raise the relative concentration of the compact isomer is decreasing, and the isomer of the  $D_{2d}$  symmetry becomes more abundant.

**Table 5. Calculated properties of superhalogens  $MgX_3$  ( $X=F, Cl$ )**

Property	B3P86 Ext	MP2 Ext	B3P86 Ext	MP2 Ext	CCSD(T)/ 6-311+G* [26]
	$MgF_3^- (D_{3h}, ^1A'_1)$		$MgCl_3^- (D_{3h}, ^1A'_1)$		
$R_e(Mg-X)$	1.823	1.821	2.277	2.267	2.280
$-E$	499.90964	499.29125	1581.02044	1579.31218	1578.95346
$VED$		7.96		6.64	6.50; 6.60 $\pm$ 0.04 <sup>a</sup>
$\omega_1(A'_1)$	470	472	282	279	279
$\omega_3(A_2'')$	243	254	166	170	176
$\omega_2(E')$	656	659	444	457	460
$\omega_4(E')$	182	177	108	104	106
	$MgF_3 (C_{2v}, ^2B_2)$		$MgCl_3 (C_{2v}, ^2A_1)$		
$R_{e1}(Mg-X_1)$	1.828		2.266		
$R_{e2}(Mg-X)$	1.839		2.281		
$\alpha_e(X_1-Mg-X)$	114.9		131.6		
$-E$	499.65484		1580.79229		
$EA_{ad}$	6.93		6.21		5.61 <sup>b</sup>
$\omega_1(A_1)$	518		360		
$\omega_2(A_1)$	449		262		
$\omega_3(A_1)$	108		68		
$\omega_4(B_1)$	541		391		
$\omega_5(B_1)$	158		105		
$\omega_6(B_2)$	161		123		

Notes: <sup>a</sup> experimental value of  $VED$  for  $MgCl_3^-$  found by photoelectron spectroscopy [25]; <sup>b</sup> theoretical value of  $EV_{ad}$  was determined in [26] for the state  $^2B_2$

**Table 6. Calculated properties of supersalts  $Na_2MgX_4$  ( $D_{2d}$  symmetry)**

Property	B3P86 Ext	MP2 Ext	B3P86 Ext	MP2 Ext
	$Na_2MgF_4$		$Na_2MgCl_4$	
$-E$	924.43906	923.03530	2365.88225	2363.023612
$R_{e1}(Na-X)$	2.094	2.071	2.552	2.521
$R_{e2}(Mg-X)$	1.892	1.878	2.369	2.345
$\alpha_e(X-Na-X)$	81.9	82.8	91.5	91.5
$\beta_e(X-Mg-X)$	93.0	93.7	101.0	100.7
$\omega_1(A_1)$	428	432	340	268
$\omega_2(A_1)$	389	374	244	253
$\omega_3(A_1)$	183	161	74	96
$\omega_4(B_1)$	104	110	62	61
$\omega_5(B_2)$	602	619	387	411
$\omega_6(B_2)$	395	376	252	256
$\omega_7(B_2)$	279	271	165	169
$\omega_8(E)$	503	521	342	360
$\omega_9(E)$	337	330	234	244
$\omega_{10}(E)$	203	207	115	114
$\omega_{11}(E)$	55	62	34	22

Note: the reducible vibrational representation breaks down into irreducible ones as follows:  
 $\Gamma = 3A_1 + B_1 + 3B_2 + 4E$



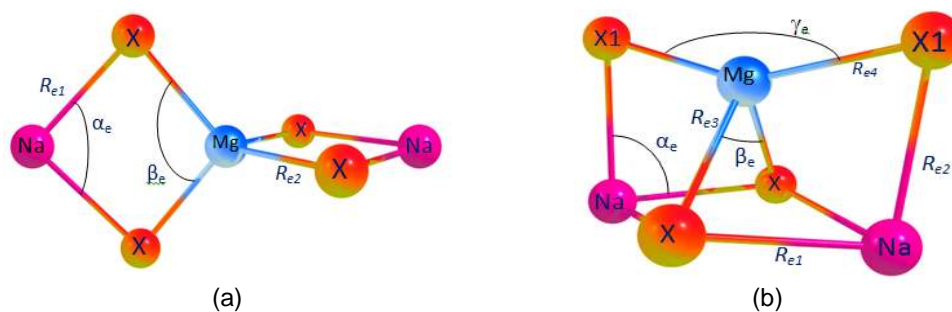


**Fig. 3. Equilibrium geometrical configurations of  $\text{Na}_2\text{MgX}_4$  isomers: (a) two-cycled structure of  $D_{2d}$  symmetry; (b) polyhedral structure of  $C_{2v}$  symmetry**

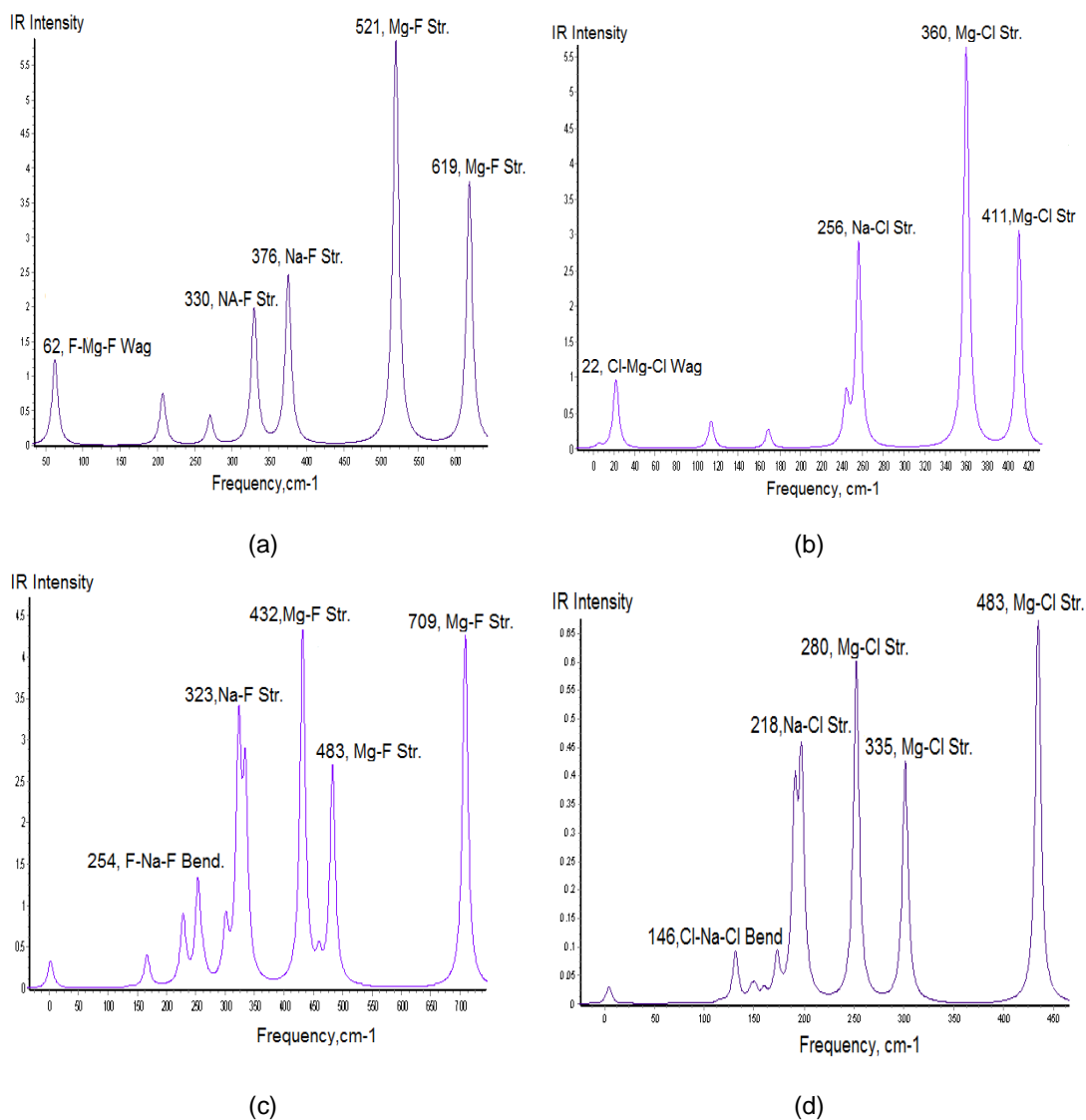


**Fig. 4. Theoretical infrared spectra (MP2 Ext) of supersalts: (a)  $\text{Na}_2\text{MgF}_4$  ( $D_{2d}$ ); (b)  $\text{Na}_2\text{MgCl}_4$  ( $D_{2d}$ ); (c)  $\text{Na}_2\text{MgF}_4$  ( $C_{2v}$ ); (d)  $\text{Na}_2\text{MgCl}_4$  ( $C_{2v}$ )**

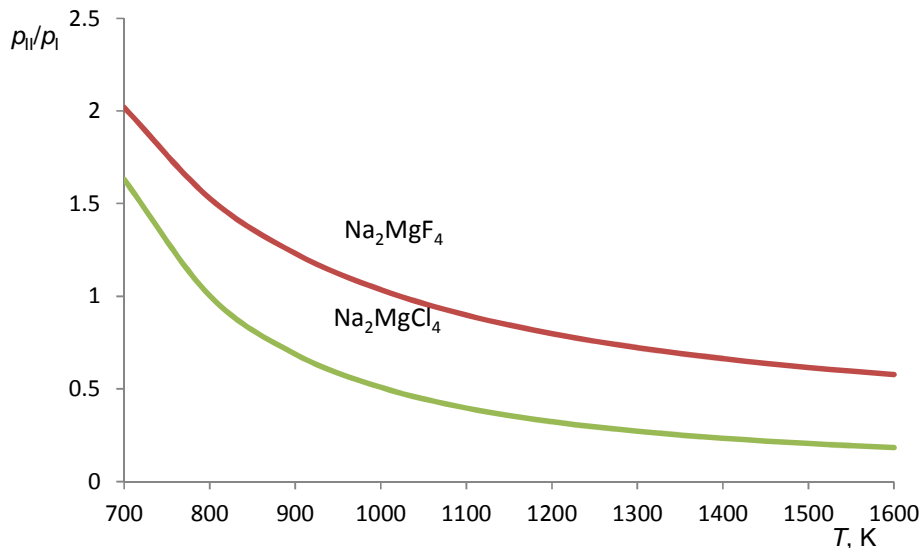


Fig. 5. Relative abundance  $p_{II}/p_I$  of two isomers of supersalts  $\text{Na}_2\text{MgF}_4$  and  $\text{Na}_2\text{MgCl}_4$ ; I is  $D_{2d}$  and II is  $C_{2v}$  isomer (MP2 Ext)

Table 7. Calculated properties of supersalts  $\text{Na}_2\text{MgX}_4$  ( $C_{2v}$  symmetry)

Property	B3P86 Ext	MP2 Ext	B3P86 Ext	MP2 Ext
	$\text{Na}_2\text{MgF}_4$		$\text{Na}_2\text{MgCl}_4$	
$-E$	924.43548	923.04024	2365.883478	2363.03220
$R_{e1}(\text{Na}-\text{X})$	2.257	2.231	2.730	2.637
$R_{e2}(\text{Na}-\text{X}_1)$	2.202	2.173	2.687	2.629
$R_{e3}(\text{Mg}-\text{X})$	1.954	1.941	2.458	2.438
$R_{e4}(\text{Mg}-\text{X}_1)$	1.842	1.825	2.301	2.286
$\alpha_e(\text{X}-\text{Na}-\text{X}_1)$	80.4	78.4	85.9	87.4
$\beta_e(\text{X}-\text{Mg}-\text{X})$	82.5	82.9	88.2	86.8
$\gamma_e(\text{X}_1-\text{Mg}-\text{X}_1)$	157.0	156.6	147.3	150.4
$\Delta_r E_{\text{iso}}$	9.4	-13.0	3.2	-22.5
$\mu_e$	6.69	6.60	7.22	6.86
$\omega_1(A_1)$	485	483	327	335
$\omega_2(A_1)$	448	460	260	271
$\omega_3(A_1)$	321	323	213	212
$\omega_4(A_1)$	305	301	183	192
$\omega_5(A_1)$	230	227	125	163
$\omega_6(A_1)$	150	139	90	99
$\omega_7(A_2)$	223	238	142	174
$\omega_8(A_2)$	134	141	86	91
$\omega_9(B_1)$	408	432	267	280
$\omega_{10}(B_1)$	236	254	134	146
$\omega_{11}(B_1)$	140	167	110	129
$\omega_{12}(B_2)$	684	709	469	483
$\omega_{13}(B_2)$	322	334	215	218
$\omega_{14}(B_2)$	267	263	168	178
$\omega_{15}(B_2)$	223	229	157	168

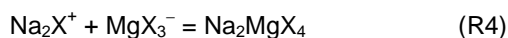
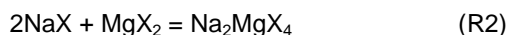
Note:  $\Delta_r E_{\text{iso}}$  are the energies of the isomerization reactions  $\text{Na}_2\text{MgX}_4 (D_{2d}) = \text{Na}_2\text{MgX}_4 (C_{2v})$ , in  $\text{kJ}\cdot\text{mol}^{-1}$ .

The reducible vibrational representation breaks down into irreducible ones as follows:

$$\Gamma = 6A_1 + 2A_2 + 3B_1 + 4B_2$$

### 3.4 Thermodynamic Properties of Supersalts

The supersalts were designed through association of different building blocks as per reactions:



The first two reactions involve the conventional salts  $\text{MgX}_2$  and  $\text{NaX}$ , and the dimer  $\text{Na}_2\text{X}_2$ , and the last two reactions involve the superhalides and superalkalies to form the supersalts. The energies  $\Delta_r E$ , zero-point vibration energy corrections  $\Delta_r \epsilon$ , and enthalpies  $\Delta_r H^\circ(0)$  of the reactions were calculated using Eqs. (1) and (2). The data obtained by DFT/B3P86 and MP2 methods with the extended basis set are presented in Table 8. For each reaction considered the difference between the  $\Delta_r H^\circ(0)$  values by B3P86 and MP2 methods is rather big, lying in the range 30–70 kJ mol<sup>-1</sup>. The calculated enthalpies of the reactions  $\Delta_r H^\circ(0)$  show that all reactions proceed with release of heat energy (i.e. exothermic), even though the magnitude differs between reactions. Thus, in the reaction involving dimers (R3) smaller energy is released, while reactions involving neutral superatoms (R5) give larger amount of energy as compared to others.

The enthalpies of formation  $\Delta_f H^\circ(0)$  of the supersalts were estimated through the formation

of enthalpies of the reactions (R2) and (R3) and the enthalpies of the reactants were taken from [14]. The values of  $\Delta_f H^\circ(0)$  are given in the last column of Table 8. To evaluate the accuracy of the results, we have considered the data obtained through two reactions (R2) and (R3) and two methods of calculations (B3P86 Ext, MP2 Ext). The results have been plotted in Fig. 6. It can be seen the oscillations of the  $\Delta_f H^\circ(0)$  values along each plot. As it was shown for the dimer molecules (Fig. 1), the averaged values of  $\Delta_f H^\circ(0)$  for different methods for the  $\text{Na}_2\text{F}_2$  and  $\text{Na}_2\text{Cl}_2$  molecules are in a good agreement with the reference data [14] accordingly. Using the same approach we have estimated the enthalpies of formation of  $\text{Na}_2\text{MgF}_4$  and  $\text{Na}_2\text{MgCl}_4$  molecules:  $-1850 \pm 30$  and  $-1170 \pm 40$  kJ·mol<sup>-1</sup>, respectively.

The thermodynamic stability of the salts was examined through Gibbs free energy for the reaction (R3) as it corresponds to the most probable channel of dissociation. The change in Gibbs free energy  $\Delta_r G^\circ(T)$  was calculated by the formula:

$$\Delta_r G^\circ(T) = \Delta_r H^\circ(T) - T\Delta_r S^\circ(T) \quad (5)$$

where  $\Delta_r H^\circ(T)$  is the enthalpy of the reaction,  $T$  is the absolute temperature;  $\Delta_r S^\circ$  is the entropy change. The required thermodynamic functions have been computed using rigid rotator-harmonic oscillator approximation, based on geometrical parameters and vibrational frequencies obtained in MP2 method with the extended basis set.

**Table 8. The energies of reactions,  $\Delta_r E$ , zero-point vibration energy corrections,  $\Delta_r \epsilon$ , enthalpies of the reactions,  $\Delta_r H^\circ(0)$ , and enthalpies of formation,  $\Delta_f H^\circ(0)$  of supersalts  $\text{Na}_2\text{MgX}_4$  ( $X = \text{F}, \text{Cl}$ ); all values are given in kJ · mol<sup>-1</sup>**

Property	$\text{Na}_2\text{MgF}_4$			$\text{Na}_2\text{MgCl}_4$			
	$-\Delta_r E$	$\Delta_r \epsilon$	$-\Delta_r H^\circ(0)$	$-\Delta_r E$	$\Delta_r \epsilon$	$-\Delta_r H^\circ(0)$	$-\Delta_f H^\circ(0)$
<b>R2</b>	<b><math>2\text{NaX} + \text{MgX}_2 = \text{Na}_2\text{MgX}_4</math></b>						
B3P86 Ext	514.1	10.5	503.6	1825	380.9	6.5	374.4
MP2 Ext	570.8	11.5	559.3	1881	453.5	6.8	446.7
<b>R3</b>	<b><math>\text{Na}_2\text{X}_2 + \text{MgX}_2 = \text{Na}_2\text{MgX}_4</math></b>						
B3P86 Ext	276.5	5.1	271.3	1835	188.5	3.9	184.6
MP2 Ext	311.7	4.6	307.1	1870	238.9	3.5	235.5
<b>R4</b>	<b><math>\text{Na}_2\text{X}^+ + \text{MgX}_3^- = \text{Na}_2\text{MgX}_4</math></b>						
B3P86 Ext	528.5	1.0	527.5		457.2	-0.8	456.4
MP2 Ext	573.1	1.6	571.5		504.3	-1.1	503.2
<b>R5</b>	<b><math>\text{Na}_2\text{X} + \text{MgX}_3 = \text{Na}_2\text{MgX}_4</math></b>						
B3P86 Ext	819.2	6.5	812.7		645.3	-4.4	640.9
MP2 Ext	802.7				597.0		

For the salts considered here the thermodynamic functions are listed in Tables A and B of the Appendix. In the  $\Delta_r G^\circ(T)$  calculations, the compact structure of  $C_{2v}$  symmetry for  $Na_2MgX_4$  obtained by MP2 with extended basis set was considered. The graph of  $\Delta_r G^\circ(T)$  vs  $T$  is shown on the Fig. 7. As is seen the values are negative in a broad temperature range, i.e. this result satisfies the condition that the reaction for the salt formation is spontaneous.

The spontaneous dissociation of the supersalts starts at the elevated temperatures: at  $\sim 2000$  K for  $Na_2MgF_4$  and  $\sim 1400$  K for  $Na_2MgCl_4$ . The

$\Delta_r G^\circ$  values indicate the thermodynamic stability of the supersalts and correlate to the enthalpies of the reactions R3 given in Table 8. For the fluoride the values of  $\Delta_r G^\circ$  are negative at a broader temperature range as compared to chloride, and the enthalpy of reaction R3 for the fluoride is more negative. The lower thermodynamic stability of  $Na_2MgCl_4$  as compared to  $Na_2MgF_4$  is accounted for stronger chemical bonds in the latter. The spontaneous course for other reactions (R2, R4, and R5) is predictable as the enthalpies of these reactions are even more negative than for R2.

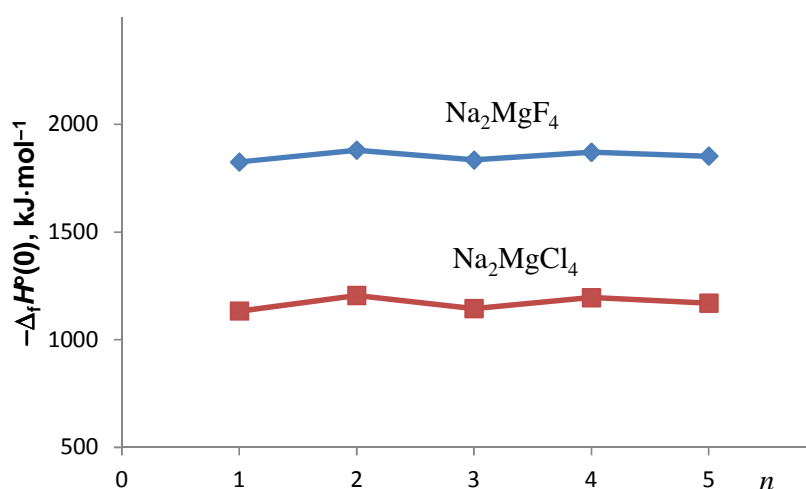


Fig. 6. The enthalpies of formation of the salts calculated through different approaches:  $n = 1, 2$  correspond to reaction  $2NaX + MgX_2 = Na_2MgX_4$  (1 – B3P86 EXT, 2 – MP2 EXT);  $n = 3, 4$  correspond to reaction  $Na_2X_2 + MgX_2 = Na_2MgX_4$  (3– B3P86 EXT, 4– MP2 EXT);  $n = 5$  correspond to the averaged values

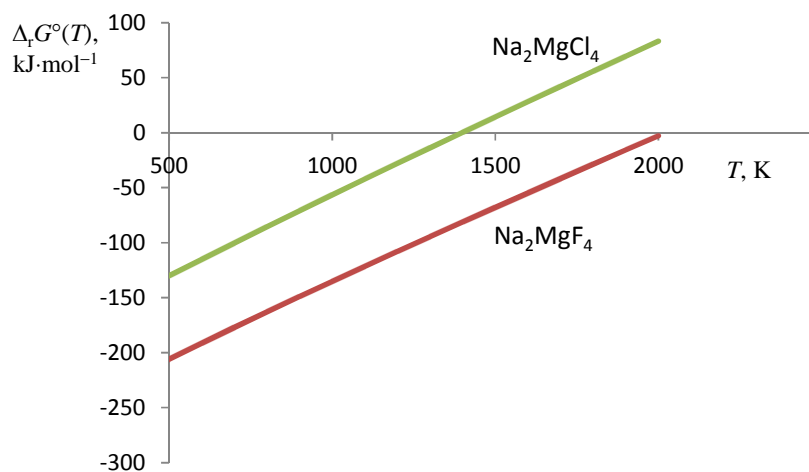


Fig. 7. Gibbs free energy change against temperature for reaction  $Na_2X_2 + MgX_2 = Na_2MgX_4$ ; the polyhedral isomer ( $C_{2v}$ ) for  $Na_2MgX_4$  was considered

#### 4. CONCLUSION

The geometrical parameters and vibrational frequencies of superalkalies  $\text{Na}_2\text{X}$ , superhalogens  $\text{MgX}_3$ , dimers  $\text{Na}_2\text{X}_2$  and supersalts  $\text{Na}_2\text{MgX}_4$  ( $\text{X} = \text{F}, \text{Cl}$ ) have been determined using DFT/B3P86 and MP2 methods. The results obtained by DFT and MP2 methods do not contradict each other and the available reference data. The low ionization energies of the superalkalies and high electron affinities of superhalogens not only suggest their suitability as building blocks but also predict the stability and existence of the supersalts they compose.

For the supersalts  $\text{Na}_2\text{MgF}_4$  and  $\text{Na}_2\text{MgCl}_4$ , two isomers; polyhedral ( $C_{2v}$ ) and two-cycled ( $D_{2d}$ ), were proved to exist; the relative concentrations of the isomers in equilibrium vapour were evaluated and found to be comparable at  $\sim 1000$  K. The enthalpies and Gibbs energies of association reactions indicated the thermodynamic stability of the supersalts and spontaneity for the salt formation process in a broad temperature range.

The supersalts considered are predicted to be useful in catalysis, ion batteries manufacturing and design of novel functional materials. Therefore this study is not only anticipated to widen the theoretical understanding of supersalts but also to provide sound promises and calls to experimentalists and technologists to come out with tangible novel supersalts and its derivatives.

#### ACKNOWLEDGEMENT

The authors are very thankful to the government of Tanzania through The Nelson Mandela African Institution of Science and Technology for supporting and sponsoring this research work.

#### COMPETING INTERESTS

Authors have declared that no competing interests exist.

#### REFERENCES

1. Wang XB, Ding CF, Wang, LS, Boldyrev, AI, Simons J. First experimental photoelectron spectra of superhalogens and their theoretical interpretations. *J. Chem. Phys.* 1999;110(10).
2. Khanna SN, Jena P. Atomic clusters: Building blocks for a class of solids. *Phys. Rev. B.: Condens. Matter.* 1995;51:13705-13716:3.
3. Gutsev GL, Boldyrev AI. DVM-Xa calculations on the ionization potentials of  $\text{M}_{k+1}\text{X}$  -complex anions and the electron affinities of  $\text{MX}_{k+1}$  "superhalogens". *J.Chem. Phys.* 1981;56(3):277-283.
4. Tian W, Yang K, Li Q, Li W, Cheng J. Hydrogen bonding involved with superhalogens  $\text{MX}_2\text{NY}$ : Its influence on the structure and stability of the superhalogens. *Molecular Physics.* 2014; 112(15):1947-1953.
5. Srivastava AK, Misra N. Novel  $\text{Li}_3\text{X}_3$  supersalts ( $\text{X} = \text{F}, \text{Cl}, \text{Br} \ \& \ \text{I}$ ) and their alkalide characteristics. *New J. Chem;* 2014;38(7):2890-2893.
6. Giri S, Behera S, Jena P. Superalkali and superhalogens as building blocks of supersalts. *J. Chem. Phys.* 2014;118(3): 638-645.
7. Schmidt MW, Baldrige KK, Boatz JA, Elbert ST, Gordon MS, Jensen JH, Koseki S, Matsunaga N, Nguyen KA, Su S, Windus TL, Dupuis M, Montgomery JA. General Atomic and Molecular Electronic Structure System. *J Comput. Chem.* 1993; 14:1347-1363. DOI:10.1002/jcc.540141112.
8. Granovsky AA. Firefly version 8.1.0, www.2014. Accessed 15 March 2015. Available:<http://classic.chem.msu.su/gran/firefly/index.html>
9. Feller D, The role of databases in support of computational chemistry calculations *Comput. Chem.* 1996;17(13):1571-1586.
10. Schuchardt KL, Didier BT, Elsethagen T, Sun L, Gurumoorthi V, Chase J, Li J, Windus TL, Basis set exchange: a community database for computational sciences. *J. Chem. Inf. Model.* 2007;47(3): 1045-1052.
11. Basis set library EMSL (The Environmental Molecular Sciences Laboratory, U.S.) Available:<https://bse.pnl.gov/bse/portal>
12. Chemcraft. Version 1.7 (build 132). GA Zhurko, Zhurko DA. Available:[www.chemcraftprog.com](http://www.chemcraftprog.com)
13. Tokarev KL. "Open Thermo", v.1.0 Beta 1 (C); 2007-2009. Available:<http://openthermo.software.informer.com/>
14. Gurvich LV, Yungman VS, Bergman GA, Veitz IV, Gusarov AV, Iorish VS, Leonidov VY, Medvedev VA, Belov GV, Aristova NM, Gorokhov LN, Dorofeeva OV, Ezhov

- YS, Efimov ME, Krivosheya NS, Nazarenko II, Osina EL, Ryabova VG, Tolmach PI, Chandamirova NE, Shenyavskaya EA. Thermodynamic properties of individual substances. Ivtanthermo for windows database on thermodynamic properties of individual substances and thermodynamic modeling software, Version 3.0 (Glushko Thermocenter of RAS, Moscow; 1992–2000.
15. Available:[http://www.ccl.net/cca/document/s/dyoung/topics-orig/spin\\_cont.html](http://www.ccl.net/cca/document/s/dyoung/topics-orig/spin_cont.html)
  16. Jensen F. A remarkable large effect of spin contamination on calculated vibrational frequencies. *Chemical Physics Letters*. 1990;169(6):519-528.
  17. Huber KP, Herzberg G. Constants of diatomic molecules (data prepared by JW Gallagher and RD Johnson, III) in *NIST Chemistry WebBook*, NIST Standard Reference Database Number 69, eds. PJ Linstrom and WG Mallard; 2001.
  18. Gurvich LV, Veyts IV, Alcock CB, Eds., *Thermodynamic properties of individual substances*, 4<sup>th</sup> ed., Hemisphere Publishing Corp., New York; 1989.
  19. NIST Chemistry Webbook. Available:<http://webbook.nist.gov/chemistry>
  20. Jacox ME. Vibrational and electronic energy levels of polyatomic transient molecules. Supplement B. *J. Phys. Chem. Ref. Data*. 2003;32(1):1-441.
  21. Hargittai M. Molecular structure of metal halides. *Chem. Rev.* 2000;100(6):2233-2302.
  22. Snelson A, Cyvin SJ, Cyvin BN. Infrared spectrum of LiNaF<sub>2</sub>. *J. Phys. Chem.* 1970; 74(25):4338-4343.
  23. Ismail ZK, Hauge RH, Margrave JL. Infrared studies of matrix isolated sodium and potassium chloride and cyanide dimers. *Journal of Molecular Spectroscopy*. 1975;54(3):402-411.
  24. Pogrebnaya TP, Pogrebnoi AM, Kudin LS. Calculation of the thermodynamic characteristics of ions in vapor over sodium fluoride. *Russ.J. Phys. Chem. A*, 2008;82(1):75-82.
  25. Pogrebnaya TP, Pogrebnoi AM, Kudin LS. Theoretical study of the structure and stability of the Na<sub>2</sub>Cl<sup>+</sup>, NaCl<sub>2</sub><sup>-</sup>, Na<sub>3</sub>Cl<sub>2</sub><sup>+</sup>, and Na<sub>2</sub>Cl<sub>3</sub><sup>-</sup> ions. *J. Struct. Chem.* 2007;48(6): 987-995.
  26. Elliot BM, Koyle E, Boldyrev AI, Wang XB, Wang LS. MX<sub>3</sub><sup>-</sup> Super Halogens (B = Be, Mg, Ca; X = Cl, Br): A Photoelectron Spectroscopic and ab Initio Theoretical Study. *J. Phys. Chem. A*. 2005;109(50): 11560.  
DOI:10.1021/jp054036v

## APPENDIX

The thermodynamic functions of supersalts  $\text{Na}_2\text{MgF}_4$  and  $\text{Na}_2\text{MgCl}_4$  in gaseous phase were calculated using Openthermo software [13]. The molar heat capacity  $c_p^\circ(T)$ ; Gibbs reduced free energy  $\Phi^\circ(T)$ ; entropy  $S^\circ(T)$ ; and enthalpy increment  $H^\circ(T) - H^\circ(0)$ , in  $\text{J}\cdot\text{mol}^{-1}\cdot\text{K}^{-1}$ ,  $\text{J}\cdot\text{mol}^{-1}\cdot\text{K}^{-1}$ ,  $\text{J}\cdot\text{mol}^{-1}\cdot\text{K}^{-1}$  and  $\text{kJ}\cdot\text{mol}^{-1}$ , respectively, are listed in Table A and B. The geometrical parameter and vibrational frequencies were calculated by MP2 method with extended basis set.

Table A. Thermodynamic functions of  $\text{Na}_2\text{MgF}_4$ 

$T, \text{K}$	$c_p^\circ(T)$	$\Phi^\circ(T)$	$S^\circ(T)$	$H^\circ(T) - H^\circ(0)$	$T, \text{K}$	$c_p^\circ(T)$	$\Phi^\circ(T)$	$S^\circ(T)$	$H^\circ(T) - H^\circ(0)$
$D_{2d}$ isomer					$C_{2v}$ isomer				
298.15	134.700	302.947	396.112	27.777	298.15	135.070	292.802	383.270	26.973
700	152.900	396.450	520.512	86.844	700	152.950	384.818	507.821	86.102
800	154.050	413.265	541.009	102.195	800	154.090	401.503	528.324	101.457
900	154.850	428.489	559.202	117.642	900	154.870	416.624	546.522	116.908
1000	155.430	442.392	575.549	133.157	1000	155.460	430.445	562.871	132.426
1100	155.870	455.181	590.384	148.723	1100	155.880	443.168	577.708	147.994
1200	156.200	467.022	603.961	164.327	1200	156.220	454.955	591.287	163.599
1300	156.450	478.043	616.474	179.960	1300	156.470	465.929	603.801	179.234
1400	156.660	488.350	628.076	195.616	1400	156.680	476.196	615.404	194.891
1500	156.820	498.030	638.891	211.291	1500	156.850	485.841	626.219	210.567
1600	156.980	507.154	649.017	226.981	1600	156.990	494.935	636.346	226.258

Table B. Thermodynamic functions of  $\text{Na}_2\text{MgCl}_4$ 

$T, \text{K}$	$c_p^\circ(T)$	$\Phi^\circ(T)$	$S^\circ(T)$	$H^\circ(T) - H^\circ(0)$	$T, \text{K}$	$c_p^\circ(T)$	$\Phi^\circ(T)$	$S^\circ(T)$	$H^\circ(T) - H^\circ(0)$
$D_{2d}$ isomer					$C_{2v}$ isomer				
298.15	146.210	358.475	469.076	32.976	298.15	146.500	333.301	440.683	32.016
700	155.630	464.097	598.863	94.336	700	155.690	437.125	570.593	93.428
800	156.180	482.272	619.683	109.929	800	156.210	455.139	591.419	109.024
900	156.550	498.582	638.100	125.566	900	156.570	471.323	609.840	124.665
1000	156.800	513.374	654.609	141.235	1000	156.840	486.015	626.352	140.337
1100	157.010	526.905	669.565	156.926	1100	157.040	499.464	641.310	156.031
1200	157.170	539.371	683.234	172.636	1200	157.190	511.862	654.980	171.742
1300	157.280	550.927	695.819	188.359	1300	157.310	523.362	667.567	187.467
1400	157.440	561.698	707.478	204.092	1400	157.400	534.083	679.227	203.202
1500	157.490	571.783	718.339	219.834	1500	157.470	544.126	690.089	218.945
1600	157.520	581.264	728.503	235.583	1600	157.550	553.570	700.254	234.695

© 2016 Ulime et al.; This is an Open Access article distributed under the terms of the Creative Commons Attribution License (<http://creativecommons.org/licenses/by/4.0>), which permits unrestricted use, distribution, and reproduction in any medium, provided the original work is properly cited.

Peer-review history:

The peer review history for this paper can be accessed here:  
<http://sciencedomain.org/review-history/11672>